

# High-Speed Optical Phased Array

## Using High-Contrast Grating All-Pass Filters

Weijian Yang<sup>1</sup>, Tianbo Sun<sup>1</sup>, Yi Rao<sup>1</sup>, Mischa Megens<sup>2</sup>, Trevor Chan<sup>2</sup>, Byung-Wook Yoo<sup>1</sup>, David A. Horsley<sup>2</sup>, Ming C. Wu<sup>1</sup>, and Connie J. Chang-Hasnain<sup>1,\*</sup>

<sup>1</sup> Department of Electrical Engineering and Computer Sciences, University of California at Berkeley, Berkeley, California 94720, United States

<sup>2</sup> Department of Mechanical and Aerospace Engineering, University of California at Davis, Davis, California 95616, United States

\*Email: [cch@eecs.berkeley.edu](mailto:cch@eecs.berkeley.edu)

**Abstract** — A novel optical phased array is experimentally demonstrated with high speed (0.577 MHz) beam steering, which consists of 8x8 tunable 1550-nm all-pass filters with ultrathin high-contrast grating as the micro-electro-mechanically actuated reflector for fast tuning.

**Index Terms** — Beam steering, gratings, metamaterials, microelectromechanical devices, optical devices, optical phased arrays.

### I. INTRODUCTION

Optical phased array for free-space beam steering has been of intense research interests for a wide range of applications, e.g. imaging, display, chemical-bio sensing, precision targeting, surveillance, etc. Chip-scale optical phased array is desirable due to their integration capability, small footprint, and low power consumption. Several phase tuning mechanisms have been demonstrated using electro-mechanical [1], electro-optic [2], thermo-optic effect [3], etc. However, most of them are relatively slow at a few kHz to tens of kHz. Tuning in the order of MHz is critical to enable the advanced application in light detection and ranging (LIDAR) as well as optical circuit switching.

In this paper, we experimentally demonstrate a novel 8x8 optical phased array with high-speed micro-electro-mechanical actuation. Each array element is a tunable all-pass filter (APF) with high-contrast near-wavelength grating (HCG) [4, 5] as the top reflector and distributed Bragg reflector (DBR) as the bottom reflector. An HCG is a single layer of high-index material fully surrounded by low-index material with the period less than one wavelength, which can be designed to have broadband surface-normal reflection. An all-pass filter is an asymmetric Fabry-Perot (FP) etalon with carefully designed top and bottom reflectivities such that, when tuned across the FP resonance, the reflected light experiences continuous phase change approaching  $2\pi$  without significant change of reflectivity. The APF enables a high efficiency phase tuning with small actuation distance. The ultrathin light-weight HCG further ensures a high tuning speed.

### II. HCG ALL-PASS FILTER OPTICAL PHASED ARRAY

#### A. HCG All-Pass Filter Design and Characterization

Figure 1 shows the schematics of an individual array element. The HCG is fabricated on a p-Al<sub>0.6</sub>Ga<sub>0.4</sub>As epitaxial layer, which is on top of a sacrificial layer and 22 pairs of GaAs/Al<sub>0.9</sub>Ga<sub>0.1</sub>As n-DBR. With the sacrificial layer subsequently etched, the suspended HCG and bottom DBR forms a tunable Fabry-Perot cavity. We design the HCG period ( $\Lambda$ ), bar width ( $s$ ) and thickness ( $t_g$ ) to be 1150 nm, 700 nm and 450 nm respectively, such that its reflectivity is  $\sim 90\%$ . The incident light polarization is TE, i.e. electrical field along the HCG bars. The static cavity length is 700 nm, corresponding to a resonance wavelength  $\sim 1550$  nm. The optical phased array is composed of 8x8 individual pixels. Each HCG mirror size is 20  $\mu\text{m}$  by 20  $\mu\text{m}$ ; the pitch is  $\sim 28.5\mu\text{m}$ . Figure 2 shows the scanning electron microscope (SEM) image of the fabricated device.

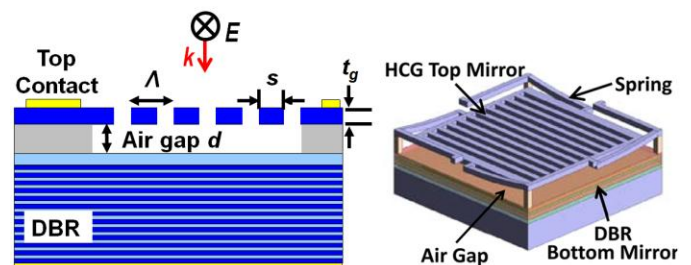


Fig. 1 Schematic of an individual pixel of the optical phased array. The Al<sub>0.6</sub>Ga<sub>0.4</sub>As HCG and 22 pairs of GaAs/Al<sub>0.9</sub>Ga<sub>0.1</sub>As DBR serve as the top and bottom reflector of the Fabry-Perot etalon. The incident light's polarization is parallel to the grating bar.  $\Lambda$ , HCG period;  $s$ , grating bar width;  $t_g$ , HCG thickness;  $d$ , air gap between HCG and DBR.

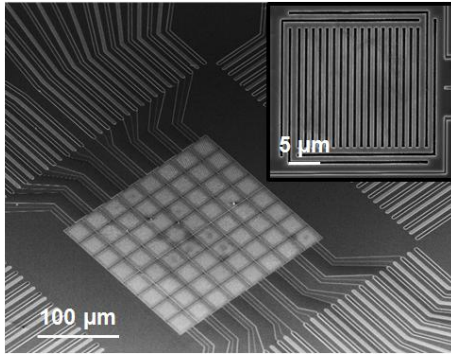


Fig. 2 SEM image of the fabricated device. The HCG array consists of 8x8 pixels. Groups of four pixels are electrically connected to increase the fill-factor. Inset, zoomed-in image of an individual pixel.

The HCG can be actuated by applying a reverse electrical bias between the HCG and DBR. This changes the cavity length and thus the reflection phase. Figure 3 shows the reflection phase of an individual etalon versus applied voltages, measured with an interferometer. A total of  $\sim 1.75\pi$  phase change is achieved with a very small actuation voltage, corresponding to an actuation distance of the HCG  $\sim 10$  nm (calculated from Fig. 4). This is expected for the all-pass filters with high quality factor (Q).

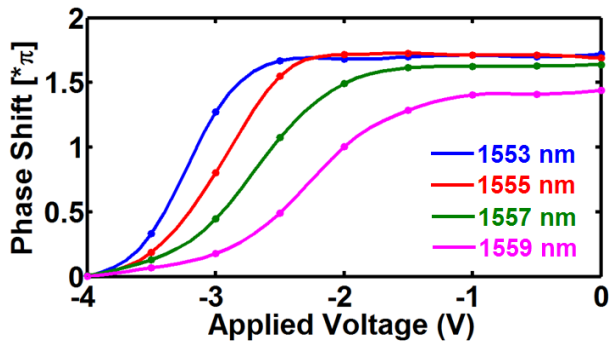


Fig. 3 Reflection phase shift versus applied voltage on an individual pixel of the phased array.  $\sim 1.75\pi$  phase shift is achieved with small actuation voltage range. As the incident wavelength increases, the resonance cavity length increases, and thus less voltage is needed to actuate the HCG to reach the resonance cavity length. This all-pass filter design enables a small actuation distance and thus fast tuning speed. The dots on the curves are the experimental sampling points. The curves are the fitting results using smoothing-spline algorithm.

By tuning the cavity resonance wavelength through different applied voltages, this all-pass filter can operate in a large wavelength range. Figure 4 shows the reflection spectrum of the all-pass filter. A large reflection dip was observed, indicating a sharp resonance wavelength and thus a high quality factor. Based on the reflection spectrum of all 64 pixels, Q value is estimated to be 170~260. The HCG reflectivity is back calculated to be 95%~98%, and the bottom DBR reflectivity is  $99.3\% \pm 0.3\%$ . The HCG reflectivity is higher than the design value of 90% due to an inadvertent inaccuracy in electron beam lithography and etching process.

Nevertheless, the Q value is in good agreement with the calculated value based on actual HCG dimensions measured by SEM.

The resonance wavelength can be extracted for each applied voltage on Fig. 4. As the reverse-bias voltage amplitude increases, the cavity length decreases, resulting in a blue shift of the resonance wavelength. Based on the round trip phase condition of the cavity resonance, the actuation distance of the HCG can be calculated for each applied voltage. At an applied voltage of -4V, the actuation distance is  $\sim 10$  nm.

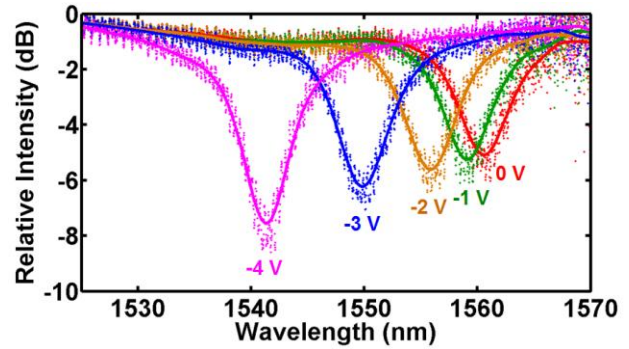


Fig. 4 Reflection spectrum of an individual pixel of the phased array for different applied voltages. The large and sharp resonance dip indicates a high quality factor. As the reverse-bias voltage amplitude increases, the cavity length decreases, resulting in a blue shift of the resonance wavelength. The resonance wavelength can be extracted for each applied voltage. Based on the round trip phase condition of the cavity resonance, the actuation distance of the HCG can be calculated for each applied voltage. With the reflection spectrum of all 64 pixels, Q value is estimated to be 170~260. The dots on the curves are the experimental sampling points. The curves are the fitting results using smoothing-spline algorithm.

### B. Beam Steering Experiment

The desired reflection phase front of the HCG array can be created by individually applying different voltages to different pixels; the reflected beam can thus be steered. The HCG bar is  $45^\circ$  aligned to the input beam's polarization, and thus the HCG sees both TE and TM polarization. Only TE polarization can be steered. TM polarization does not "see" the cavity effect due to a very low HCG reflectivity ( $\sim 30\%$ ). Its reflection phase does not change with applied voltage, and it contributes to the non-steered beam. The reflection beam then passes through a polarizer,  $90^\circ$  oriented to the incident light's polarization. This eliminates the background reflection. The steered beam's angle is further amplified by a lens pair. Figure 5 shows the far field intensity distribution of the steered beam, in good agreement with the simulation results. The energy of TM polarization is subtracted from the 0<sup>th</sup> order beam. Since only a very small actuation distance is needed for large phase shift, the beam steering bandwidth can be estimated by the mechanical resonance frequency  $f_r$  of the HCG actuation, measured by laser Doppler velocimetry.  $f_r$  is  $\sim 0.39$  MHz for the current array, thanks to the light weight of the HCG mirror

( $\sim 0.67$  ng). A shorter spring design has yielded an  $f_r$   $\sim 0.577$  MHz, shown in Fig. 6. Bandwidth in excess of 1 MHz can be achieved by the optimization of the micro-electro-mechanical design.

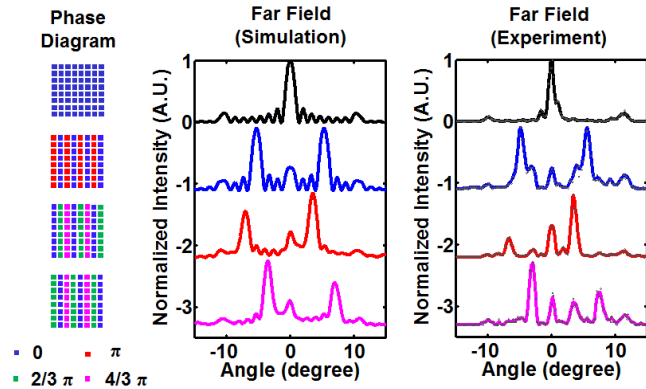


Fig. 5 Beam steering experiment. The experimental results are well-matched with simulation results. The discrepancy is due to some non-uniformity of the HCG array. The TM polarized light experiences a very low Q etalon, and thus its reflection phase does not change with applied voltage. It contributes to the 0<sup>th</sup> order beam. The TM light's energy is thus subtracted from the 0<sup>th</sup> order beam.

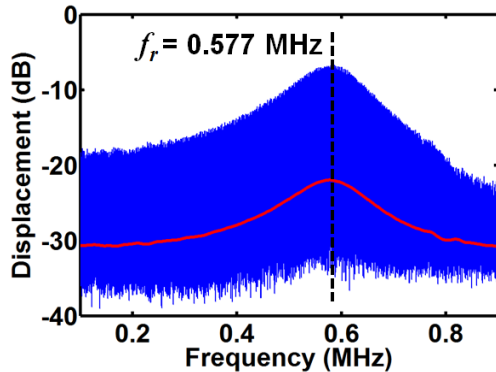


Fig. 6 Mechanical resonance  $f_r$  measured by laser Doppler velocimetry.  $f_r$  can be increased by optimization of the micro-electro-mechanical design of the individual pixel.

### III. SUMMARY

We experimentally demonstrate a novel high speed optical phased array for beam steering based on the micro-electro-mechanically actuated HCG all-pass filter array. A large optical phase tuning ( $\sim 1.75 \pi$ ) is achieved by a small actuation distance ( $\sim 10$  nm) of the ultrathin lightweight HCG mirror. This enables a high efficiency and high speed (0.577 MHz) beam steering. Optimization of the HCG all-pass filter and the micro-electro-mechanical structure will further improve the beam steering quality and increase its operation bandwidth.

### ACKNOWLEDGEMENT

We thank the support of DARPA SWEEPER Program (No. HR0011-10-2-0002) and a Guggenheim Fellowship (CCH).

### REFERENCES

- [1] U. Krishnamoorthy, K. Li, K. Yu, D. Lee, J. P. Heritage, and O. Solgaard, "Dual-mode micromirrors for optical phased array applications," *Sens. Actuators A, Phys.*, vol. 97-98, pp. 21-26, April 2002.
- [2] Q. W. Song, X.-M. Wang, R. Bussjager, and J. Osman, "Electro-optic beam-steering device based on a lanthanum-modified lead zirconate titanate ceramic wafer," *App. Opt.*, vol. 35, no. 17, pp. 3155-3162, June 1996.
- [3] J. K. Doylend, M. J. R. Heck, J. T. Bovington, J. D. Peters, L. A. Coldren, and J. E. Bowers, "Two-dimensional free-space beam steering with an optical phased array on silicon-on-insulator," *Opt. Express*, vol. 19, no. 22, pp. 21595-21604, October 2011.
- [4] C. J. Chang-Hasnain, Y. Zhou, M. C. Y. Huang, C. Chase, "High-contrast grating VCSELs," *IEEE J. Sel. Topics Quantum Electron.*, vol. 15, no. 3, pp. 869-878, May/June 2009.
- [5] C. J. Chang-Hasnain, "High-contrast gratings as a new platform for integrated optoelectronics," *Semicond. Sci. Technol.*, vol. 26, no.1, 014043, January 2011.